Numerical Simulation of Rockburst Characteristics of Tunnel Surrounding Rock Under Dilatancy Effect

Jian-qiang Yu, Qi Li, Yong-lu Wang, and Shuai Tao

Abstract Rockburst is one of the most intense reactions in various instability phenomena of underground cavern surrounding rock, which seriously threatens the safety of underground engineering construction personnel and equipment. Based on Mohr–Coulomb strain softening model, the non-associated flow rule is adopted for plastic flow after material yield. By implanting Gu Ming-cheng and Tao Zhen-yu rockburst criterion in the software, the effects of different dilatancy angles on rockburst grade and circumferential stress distribution of surrounding rock of circular tunnel are simulated. The calculation results show that the larger the dilatancy angle is, the more difficult the rock burst pit is to form. The elements of serious rockburst are mainly concentrated in the wall of the tunnel, and the shear bands formed in the high value area of shear strain increment are short. When the dilatancy angle is small, the circumferential stress reaches the maximum at the interface of elastic-plastic zone. With the increase of dilatancy angle, the number of elements entering the plastic state and occurring medium and severe rockburst increases first and then decreases, while the number of elements occurring slight rockburst decreases monotonously. Different dilatancy angles have significant effects on the number of elements occurring rockburst at all levels.

Keywords Dilatancy effect · Rockburst · Strain softening · Circumferential stress

J. Yu · S. Tao (✉)
POWERCHINA Huadong Engineering Corporation Limited, Hangzhou 311122, Zhejiang, China
e-mail: tao_s@hdec.com

Zhejiang Huadong Engineering Consulting Corporation Limited, Hangzhou 311122, Zhejiang, China

Q. Li
Powerchina Road Bridge Group Corporation Limited, Beijing 100048, China

Y. Wang
Sinohydro Bureau 14th Corporation, Kunming 650051, China

1 Introduction

Rockburst is one of the most intense reactions in various instability phenomena of underground cavern surrounding rock, which seriously threatens the safety of underground engineering construction personnel and equipment. At present, scholars in various countries have conducted in-depth research on the mechanism and influencing factors of rockburst in hard brittle surrounding rock with high geostress, especially the research on the early prediction of rockburst concerned by the engineering community is very active [1–3]. The research methods of rockburst prediction mainly include acoustic emission method, seismic monitoring method and the combination of the two methods. In addition, numerical methods are also widely used for rockburst prediction. With the help of appropriate rockburst criteria, numerical methods can be used to directly analyze the possibility of rockburst and the location and intensity classification of possible rock bursts, and be corrected in time with field construction [4–6]. Geotechnical materials often show volume expansion in the process of loading deformation, which will produce expansion behavior after the peak. The volume change of rock and soil mass in the shear yield process is significantly affected by the dilatancy angle.

The dilatancy angle is usually used to describe the mechanical behavior of rock and soil material after peak expansion in continuum mechanics [5–7]. Therefore, it is an important parameter to measure the volume change of rock and soil material and the expansion phenomenon, and it is one of the hot issues in geotechnical engineering. However, in theory and numerical analysis of rock mechanics, the dilatancy angle is often simplified to 0° or equal to the internal friction angle, sometimes completely ignored [6–8]. At present, in the constitutive relationship of geotechnical materials using the non-associated flow rule, the value of dilatancy angle ψ is generally smaller than that of internal friction angle φ, but the specific value is still uncertain, which is usually approximated as 0 [7–10]. On the basis of previous studies, this paper adopts Gu Ming-cheng and Tao Zhen-yu rockburst criterion [11, 12] to discuss the influence of different dilatancy angles on rockburst grade and circumferential stress distribution of surrounding rock of circular tunnel by changing the value of dilatancy angle.

2 Calculation Model, Scheme and Rock Burst Criterion

2.1 Calculation Model, Scheme and Constitutive Parameters

The length (x direction) and height (y direction) of the model are both 10 m, which are divided into 40,000 rectangular elements with the same area. Before the tunnel excavation, in order to make the calculation model reach the static equilibrium state as soon as possible, the stress of each small unit is set to be equal to the confining pressure. When the calculation reaches the equilibrium, the tunnel with a radius of

Fig. 1 Model geometry and
boundary conditions
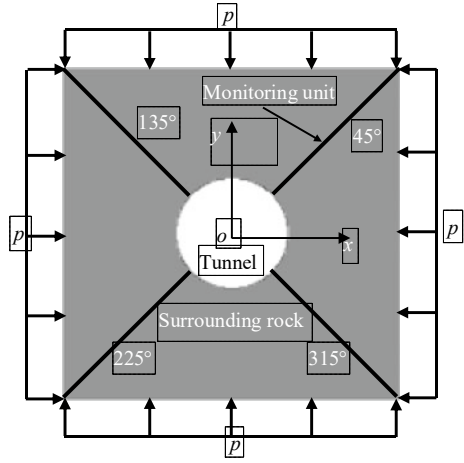
1.66 m is excavated in the model. The model after excavation is shown in Fig. 1. After tunnel excavation, the stress of surrounding rock is redistributed. When the calculation reaches 50,000 time steps, the model reaches the static equilibrium state again.

In order to study the distribution of circumferential stress of surrounding rock of tunnel, four rows of elements whose center is located on the four vertices connecting the center of tunnel to the model are selected as the monitored elements, namely, the elements in the directions of 45, 135, 225 and 315°, as shown in Fig. 1. This paper only gives the calculation results when the model reaches the static equilibrium state in each scheme.

In this paper, four calculation schemes are completed to study the influence of dilatancy angles on the rockburst and circumferential stress distribution of surrounding rock. The dilatancy angles of schemes 1–4 are 0°, 15°, 25° and 35°, respectively, and other parameters are the same, as shown in Table 1.

2.2 Rockburst Criterion

In this paper, the Gu-Tao rockburst criterion [11, 12] is used as the main stress rockburst criterion. The rockburst is divided into three levels (slight rockburst, moderate rockburst and severe rockburst), and the ratio of the maximum principal stress σ_1 to the uniaxial compressive strength of the rock σ_c is used to judge:

$$\sigma_c/\sigma_1 = 5.0 \sim 6.67 \quad \text{(slight rockburst)} \tag{1}$$

$$\sigma_c/\sigma_1 = 2.5 \sim 5.0 \quad \text{(moderate rockburst)} \tag{2}$$

Table 1 Mechanical parameters of surrounding rock

| Scheme	P/MPa	K/GPa	G/GPa	c/MPa	c_r/MPa	σ_t/MPa	σ_c/MPa	R/m	$\varphi_0/°$	$\varphi_r/°$	$\psi/°$	υ
Scheme 1	50	28.1	26.2	23.4	7.8	11.7	175	1.66	60	40	0.0	0.25
Scheme 2	50	28.1	26.2	23.4	7.8	11.7	175	1.66	60	40	15	0.25
Scheme 3	50	28.1	26.2	23.4	7.8	11.7	175	1.66	60	40	25	0.25
Scheme 4	50	28.1	26.2	23.4	7.8	11.7	175	1.66	60	40	35	0.25

$$\sigma_c/\sigma_1 < 2.5 \quad \text{(severe rockburst)} \tag{3}$$

3 Result Analysis and Discussion

3.1 Influence of Dilatancy Angle on Rockburst Grade of Tunnel Surrounding Rock

Figures 2–5 show the calculation results of schemes 1–4 at 50,000 time steps, respectively. The dark area in the figure is the high value area of rockburst at all levels and shear strain increment. In Scheme 1 ($\psi = 0°$), the rockburst notchs are formed in all four quadrants by the units with rockburst at all levels. The rockburst notch formed by the units with moderate and severe rockburst are obvious. The units with moderate rockburst are distributed uniformly along the surface of the tunnel in addition to the rockburst notch. The units with severe rockburst are mainly concentrated in the position of the rockburst notch, and other positions on the surface of the tunnel are only sporadically distributed by some units, as shown in Fig. 2a–c. It can be found from Fig. 2d that the high value area of the shear strain increment of the surrounding rock of the tunnel develops into multiple shear bands, and the two shear bands converge to form a shape similar to the rockburst notch, and the position is basically consistent with the rockburst notch.

From Fig. 3a–c, it can be found that in scheme 2 ($\psi = 15°$), moderate and severe rockburst occurred only in quadrants 1, 2 and 4, where obvious rockburst notch were formed and the depth of the notchs was greater than that in scheme 1. The unit where moderate rockburst occurs is not only concentrated at the location of rockburst notch, but also evenly distributed on the surface of tunnel. The unit where serious rockburst occurs is mainly concentrated at the location of rockburst notch. The units with slight rockburst did not form rockburst notch, but some units near the top of rockburst notch occurred slight rockburst. Figure 3d shows that the high value area of the shear strain increment of the surrounding rock of the tunnel develops into several narrow and

(a) (b) (c) (d)
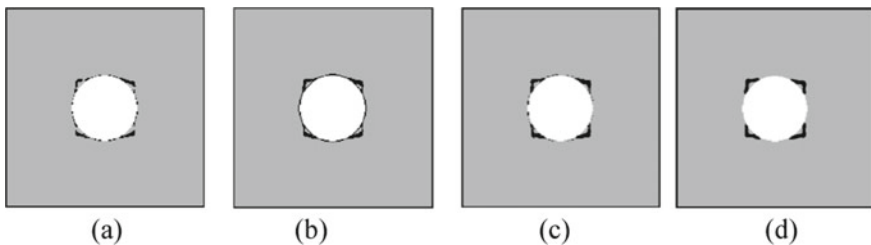
Fig. 2 Numerical results in scheme 1: **a** slight rockburst; **b** moderate rockburst; **c** serious rockburst; **d** elements having higher shear strain increments
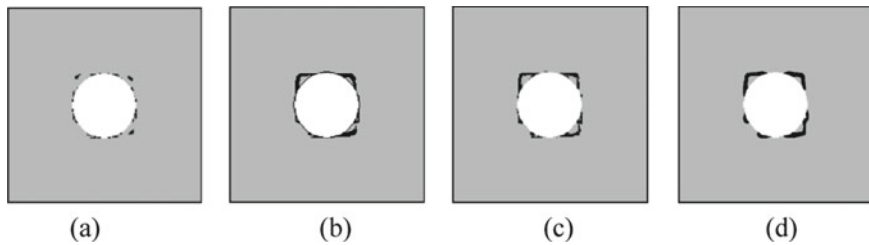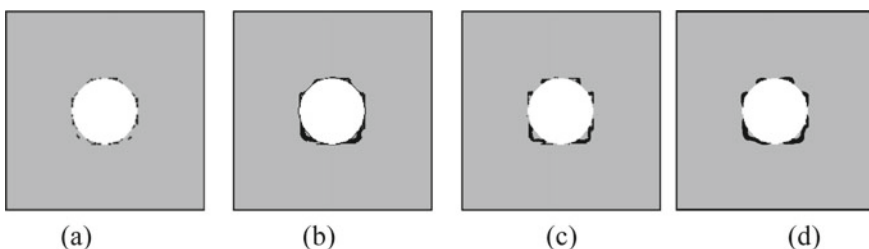
Fig. 3 Numerical results in scheme 2: **a** slight rockburst; **b** moderate rockburst; **c** serious rockburst; **d** elements having higher shear strain increments

long shear zones in the 1st, 2nd and 4th quadrants, and the two confluence forms a shape similar to the rockburst notch. However, in the 3rd quadrant, the surface distribution of the rock tunnel in the high value area of the shear strain increment does not develop into the shear zone inside the surrounding rock.
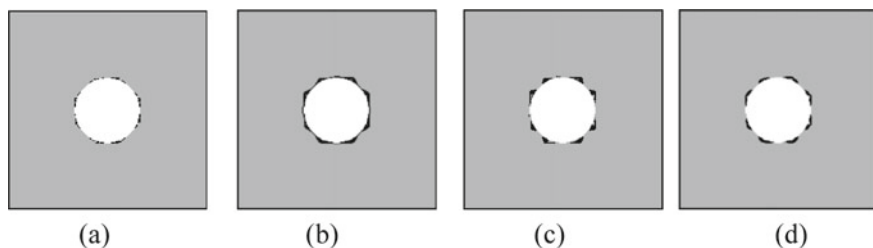
From Fig. 4a–c, it can be found that in scheme 3 ($\psi = 25°$), the moderate and severe rockburst units formed rockburst notch only in quadrants 3 and 4, and the moderate rockburst units accumulated in the surrounding rock, forming shallow rockburst notch, and the serious rockburst units formed obvious rockburst notch. In quadrants 1 and 2, the units where serious rockburst occurred did not form rockburst notch, but mainly concentrated near the top and both sides of the tunnel.

From Fig. 4d, it can be found that although the high value area of the shear strain increment of the surrounding rock of the tunnel develops into several shear zones, the shear zones distribute along the surface of the tunnel in the first and second quadrants, and do not extend to the interior of the surrounding rock to form a shape similar to that of the rockburst notch.

In the third and fourth quadrants, the shear zones are longer and slightly extend to the interior of the surrounding rock, and the two shear zones converge to form a shape similar to that of the rockburst notch formed by the unit with moderate rockburst. Compared with the results of Schemes 1 and 2, the shear bands formed by Scheme 3 are relatively smooth, and there are no obvious sharp points and corners when the two shear bands converge.

Fig. 4 Numerical results in scheme 3: **a** slight rockburst; **b** moderate rockburst; **c** serious rockburst; **d** elements having higher shear strain increments

Fig. 5 Numerical results in scheme 4: **a** slight rockburst; **b** moderate rockburst; **c** serious rockburst; **d** elements having higher shear strain increments

From Fig. 5a–c, it can be found that in scheme 4 ($\psi = 35°$), there is no rockburst notch in all levels of rockburst units. The units with slight rockburst are scattered on the surface of the tunnel, and the units with moderate rockburst are evenly distributed on the surface of the tunnel, and accumulate slightly to the interior of the surrounding rock. The units with serious rockburst are massively accumulated in the interior of the surrounding rock. It can be found from Fig. 5d that although the high value area of the shear strain increment of the surrounding rock of the tunnel develops into several short shear bands along the surface of the tunnel, its position is near the position where the unit with serious rockburst accumulates inside the surrounding rock.

3.2 Influence of Dilation on Circumferential Stress Distribution of Tunnel Surrounding Rock

Figure 6a–d show the circumferential stress distribution of the monitored units in four directions from scheme 1–scheme 4, where the ordinate is the circumferential stress value (σ_θ) of the monitored units, and the abscissa is the distance (R) from the center of the monitored units to the center of the tunnel.

From Fig. 6a, it can be found that in scheme 1 ($\psi = 0°$), the circumferential stress distribution curves of the monitored units in four directions have large fluctuations. Before reaching the maximum value, the absolute value of the circumferential stress decreases to 0 MPa, then increases to the peak value, and finally decreases and gradually tends to a certain value.

It can be found from Fig. 2a–c that all the monitored units pass through the area where the rock burst notch is located, and the units in the elastic state inside the notch are unloaded due to rockburst. Therefore, the distribution law of the annular stress of the monitored unit is shown in Fig. 6.

It can be found from Fig. 6b that in scheme 2 ($\psi = 15°$), the circumferential stress distribution curves of the monitored units in the directions of 45, 135 and 315° show obvious fluctuations. Similar to the results in scheme 1, the absolute value of circumferential stress first decreases, then increases to the peak, and finally decreases and gradually tends to a certain value.
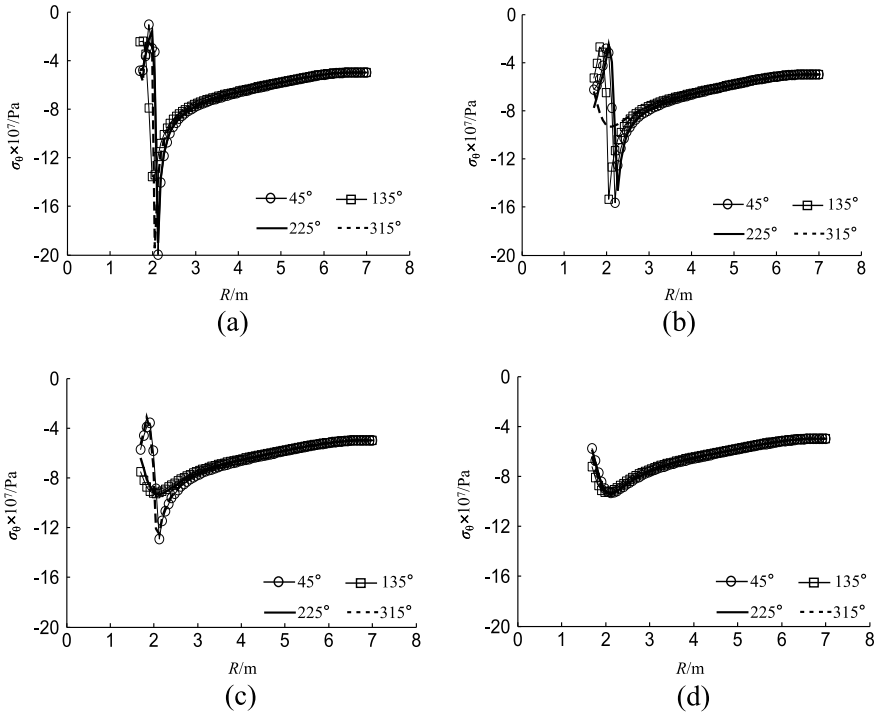
Fig. 6 Tangential stress distribution of monitored elements under different schemes: **a** scheme 1; **b** scheme 2; **c** scheme 3; **d** scheme 4

The fluctuation of circumferential stress distribution curve in scheme 2 is smaller than that in scheme 1, and the minimum value and maximum value of absolute value are between the minimum and maximum values in scheme 1. When the monitored unit in the direction of 225° is near the surface of the tunnel, the absolute value of the circumferential stress increases monotonically. With the increase of the distance from the center of the monitored units to the center of the cavern, the circumferential stress gradually tends to a certain value. From Fig. 3a–c, it can be found that the rockburst units are mainly concentrated in the first, second and fourth quadrants of the model, where the monitored unit passes through the area where the rockburst notch is located. The monitored unit located in the notch is similar to that in scheme 1, and is also unloaded due to rockburst. Therefore, the circumferential stress distribution curve will have the results shown in Fig. 6b.

From Fig. 6c, it can be found that in scheme 3 ($\psi = 25°$), only the circumferential stress distribution curves of the monitored units in 225 and 315° directions appear fluctuations similar to those in scheme 1 and 2. The absolute value of the circumferential stress of the unit near the surface of the tunnel first decreases to the minimum, then increases to the maximum, and finally decreases and gradually tends to a certain value. Compared with the first two schemes, the number of elements with reduced

Fig. 7 The number of damage units distribution in all schemes
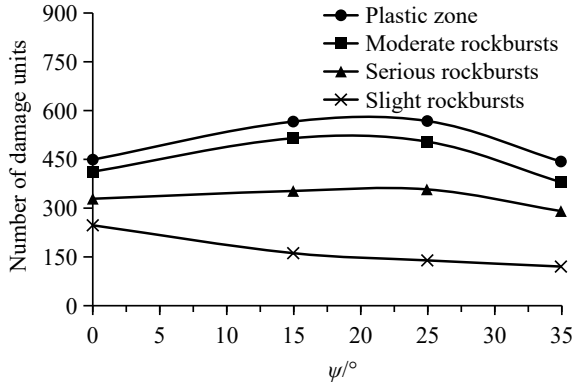
circumferential stress absolute value is reduced. From Fig. 4a–c, it can be found that the rockburst notch is formed only in the third and fourth quadrants, but the rockburst notch is shallow, and there are few monitored units in the elastic state in the notch. However, in the first and second quadrants, no rockburst notch is formed, and only the units on the surface of the tunnel have rockburst, so the distribution curve of the circumferential stress of the monitored unit will appear the result shown in Fig. 6c.

It can be found from Fig. 6d that in Scheme 4 ($\psi = 35°$), the overall trend of the circumferential stress distribution curve of the monitored unit in four directions is basically the same, which is relatively smooth and has no obvious fluctuation. It can be found from Fig. 6a–c that no rockburst notch is formed in the four quadrants of the model for the units with rockburst at all levels. Most of the monitored units in the four directions do not enter the plastic state, and rockburst occurs only in the units near the surface of the cavern. Therefore, the distribution curve of the circumferential stress of the monitored units will appear as shown in Fig. 6d.

Figure 7 gives the distribution curves of the number of elements entering the plastic state and causing minor, moderate and severe rockburst in the surrounding rock of tunnels in schemes 1 to 4. It can be found that with the increase of the dilatancy angle, the number of elements entering the plastic state and causing moderate and severe rockburst increases first and then decreases. When $\psi = 25°$, the number of elements entering plastic state and serious rockburst is the largest. When $\psi = 15°$, the largest number of units were moderate rockburst. When $\psi = 35°$, the minimum number of elements entering the plastic state, moderate and severe rockburst occurred. With the increase of dilatancy angle, the number of units with slight rockburst decreases monotonously, and when $\psi = 35°$, reaches the minimum.

4 Conclusions

Gu Ming-cheng and Tao Zhen-yu (Gu-Tao) rockburst criterion is introduced into numerical calculation to simulate the rock burst process of circular tunnel

surrounding rock with different dilatancy angles. The influence of dilation on the rockburst grade of surrounding rock and the circumferential stress distribution of surrounding rock is analyzed and discussed. The calculation results show that the larger of the dilatancy angle, the more difficult to form rockburst notch, and the more difficult of the high value region of shear strain increment to extend into surrounding rock. With the increase of dilatancy angle, the elements that cause serious rockburst will accumulate near the surface of the tunnel, and the shear band formed by the high value area of shear strain increment is shorter. When the dilatancy angle is small, because the monitored unit passes through the area where the rockburst notch is located, the hoop stress value of the unit near the surface of the tunnel decreases due to unloading, and the hoop stress value of the monitored unit at the junction of the elastic-plastic zone reaches the maximum.

With the increase of dilatancy angle, the number of failure units decreases, and the stress distribution curve of the monitored unit fluctuates less and smoother. The number of elements entering the plastic state and occurring medium and severe rockburst increases first and then decreases with the increase of dilatancy angle, while the number of elements occurring slight rockburst decreases monotonously. Different dilatancy angles have significant indigenous effects on the number of elements occurring rockburst at all levels. In this paper, the principal stress rockburst criterion is introduced into the calculation process, and the circumferential stress and energy criterion can be integrated in the next step. Considering the rockburst process of surrounding rock under the influence of multiple factors, the comprehensive evaluation calculation method of rockburst is finally given.

References

1. Patel S, Martin CD (2020) Impact of the initial crack volume on the intact behavior of a bonded particle model. Comput Geotech 127:1–10
2. Cabezas R, Vallejos J (2022) Nonlinear criterion for strength mobilization in brittle failure of rock and its extension to the tunnel scale. Int J Min Sci Technol. https://doi.org/10.1016/j.ijmst.2022.04.002
3. Nicksiar M, Martin CD (2012) Evaluation of methods for determining crack initiation in compression tests on low porosity rocks. Rock Mech Rock Eng 45(4):607–617
4. Perras MA, Diederichs MS (2014) A review of the tensile strength of rock: concepts and testing. Geotech Geol Eng 32(2):525–546
5. Alejano LR, Alonso E (2005) Considerations of the dilatancy angle in rocks and rock masses. Int J Rock Mech Min Sci 42(4):481–507
6. Lee YK, Pietruszczak S (2008) A new numerical procedure for elasto-plastic analysis of a circular opening excavated in a strain-softening rock mass. Tunn Undergr Space Technol 23(5):588–599
7. Zhao XG, Cai M, Cai MF (2010) A rock dilation angle model and its verification. Chin J Rock Mech Eng 29(5):970–981
8. Chandler NA (2013) Quantifying long-term strength and rock damage properties from plots of shear strain versus volume strain. Int J Rock Mech Min Sci 59:105–110
9. Walton G, Hedayat A, Kim E, Labrie D (2017) Post-yield strength and dilatancy evolution across the brittle-ductile transition in Indiana limestone. Rock Mech Rock Eng 50(7):1691–1710

10. Walton G (2018) Scale effects observed in compression testing of Stanstead granite including post-peak strength and dilatancy. Geotech Geol Eng 36(2):1091–1111
11. Gu MC (2001) Research on rockburst in Qinling railway tunnel. Res Water Resour Hydropower 3(4):19–26
12. Zhang JJ, Fu BJ (2008) Rockburst and its criteria and control. Chin J Rock Mech Eng 27(10):2034–2042